RSC Advances

This is an *Accepted Manuscript*, which has been through the Royal Society of Chemistry peer review process and has been accepted for publication.

Accepted Manuscripts are published online shortly after acceptance, before technical editing, formatting and proof reading. Using this free service, authors can make their results available to the community, in citable form, before we publish the edited article. This *Accepted Manuscript* will be replaced by the edited, formatted and paginated article as soon as this is available.

You can find more information about *Accepted Manuscripts* in the Information for Authors.

Please note that technical editing may introduce minor changes to the text and/or graphics, which may alter content. The journal's standard Terms & Conditions and the Ethical guidelines still apply. In no event shall the Royal Society of Chemistry be held responsible for any errors or omissions in this *Accepted Manuscript* or any consequences arising from the use of any information it contains.

ROYAL SOCIETY OF CHEMISTRY

www.rsc.org/advances

Cite this: DOI: 10.1039/c0xx00000x

www.rsc.org/xxxxxx

ARTICLE TYPE

Direct comparison on the structural and optical properties of metal-catalytic and self-catalytic assisted gallium nitride (GaN) nanowires by chemical vapor deposition

V. Purushothaman[a], P. Sundara Venkatesh[a], R. Navamathavan[b] and K. Jeganathan*[a]

Received (in XXX, XXX) Xth XXXXXXXXX 20XX, Accepted Xth XXXXXXXXX 20XX
DOI: 10.1039/b000000x

The structural and optical properties of GaN nanowires (NWs) grown by catalytic and self-catalytic assisted vapor liquid solid approach using chemical vapor deposition (CVD) were reported. Liquid Gallium droplets were used as the nucleation centre for the growth of self-catalyst assisted NWs, while pre-deposited Ni and Au thin films were employed as the seed layer for the catalyst assisted growth on Si (111) substrates. Electron microscopy analyses reveal that the growth rates and densities of structural defects of the NWs strong vary with the nature of the catalyst. High resolution electron microscopy and selected area electron diffraction study exhibits a high crystalline quality of Ni-catalyst assisted GaN NWs, while self-catalytic NWs contain defects such as stacking faults and cubic inclusion. Temperature dependent photoluminescence on the ensembles of NWs illustrate the absence of characteristic yellow luminescence band of GaN for Ni-assisted vapor-liquid-solid approach implying the high optical quality of GaN NWs by CVD. The results show that the quality of self-catalytic GaN NWs grown by CVD is yet to be improved for device applications.

Introduction

III-nitrides are direct band-gap compound semiconductors with high break down field which plays a vital role in current optoelectronics and high temperature high power electronics.[1,2,3] Semiconductor NWs hold a great promise as building blocks for novel devices in various areas like electronics, optoelectronics, photovoltaics, piezotronics, and thermoelectrics.[4,5,6,7] The most celebrated approach for the formation of NWs is the vapor–liquid–solid (VLS) process,[8] in which the external metal catalyst acts as the liquid forming seeds to promote the anisotropic NWs. Briefly, a thin metal layer containing substrate is preheated to form eutectic alloy and the precursors are allowed into the growth environment. The precursors dissociate at the growth temperature and incorporate into the catalyst droplet, subsequently the droplet is supersaturated with the elements and precipitate in the liquid-solid interface (substrate) to elongate as NWs.[8] A decade ago, the major modification in VLS growth is formulated in which the catalyst remains solid throughout the growth and the mechanism is termed as vapor-solid-solid (VSS) process.[9] Despite important advances and impressive results on NWs based applications, the reliance on gold and other metals in the fabrication process is a significant barrier to the advances in integration of NW. In particular, gold is forbidden element in complementary metal - oxide semiconductor (CMOS) processing, as it forms mid-gap electronic states in Si which degrades device performance.[10] Any fabrication process that relies on gold will be very difficult to integrate with CMOS beyond laboratory level.[11] In addition the widespread use of a catalyst raises the question whether some of the seed material is incorporated into the lattice of NWs and adversely affects their properties, thus preventing high performance applications.[12] Hence, there are increasing efforts to grow NWs without any metal catalyst terming as self-catalytic approach,[13,14,15,16] in which the excess of one of the materials form as the liquid droplets that may acts as the catalyst for the growth of NWs.[17,18,19,20] Depending on the growth parameters the self catalytic growth may be VLS or VSS.[21] Significant efforts have been given to the self-catalytic growth of III-V NWs such as GaAs and InP.[22,23,24,25] Nevertheless, only few reports are available in the literature for the self-catalytic growth of III-Nitride NWs by CVD.[26,27]

Despite some significant effort to detect the contamination by the catalyst material, understanding the differences in the quality of the NWs grown by catalytic and self-catalytic approaches is less explored. Cheze et al[28] compared the structural and optical properties of catalyst assisted and catalyst free GaN NWs grown by molecular beam epitaxy (MBE) in which they have shown that the catalyst-free GaN NWs possesses high structural and optical quality, whereas the Ni-seeded GaN NWs contains high density of stacking faults and comparatively poor luminescence properties. From their results it is evident that the catalyst assisted GaN NWs grown at lower temperature (750°C) tends to have higher stacking fault related defects. In addition they have also suggested that the Ni incorporation in GaN NWs could be the possible reason for the poor optical quality of NWs. On the other hand high temperature growth of catalyst assisted GaN NWs by other techniques such as MOCVD shows very high structural quality, as compared with the catalyst assisted MBE NWs.

RSC Advances Accepted Manuscript

However, CVD is an inexpensive and simple method to grow NWs by both catalytic and self-catalytic approach as compared to MBE and MOCVD. Hence we made an attempt to compare the structural and optical properties of GaN NWs grown by both pathways with identical growth conditions in order to deduce the effect of the catalyst. Ni-assisted GaN NWs demonstrates excellent optical properties than the Au-catalyst and self-catalytic assisted GaN NWs.

Experimental Section

GaN NWs were fabricated by the direct reaction of metal Ga (ALFA ACEAR - 99.999%) and ammonia (NH_3- 99.999%) in the horizontal CVD reactor. For both the catalyst and self-catalyst assisted growth types, Si(111) has been used as the substrates. Prior to loading, the substrates were cleaned by standard RCA procedure and 5 nm thin metal layers (Au or Ni) were deposited by e-beam evaporation method with the base vacuum of $1x10^{-6}$ mbar for catalyst assisted growth. Metal Ga of 0.1 gm is taken in a quartz crucible and placed in the alumina boat. Si substrates were kept downstream to the source Ga with the distance of 10 mm. Then the alumina boat is inserted into the growth reactor. The reactor is evacuated 10^{-3} mbar and filled with nitrogen (N_2-99.999%). N_2 gas is allowed to flow for two hours before the growth in order to overcome the residual oxygen. The temperature of the furnace is increased to the growth temperature of 900ºC at a rate of at 15ºC/min. N_2 and NH_3 flow of 500 and 200 SCCM (standard cubic centimeter), respectively is used as carrier and reactant gases. A detailed growth process for both the catalytic and self-catalytic approach has already been published elsewhere.[26,27,29] In short, for self-catalytic GaN NWs, initially N_2 is flown for 2 min to transport Ga vapor to deposit the Ga droplet layer on the Si substrate that acts as the catalyst for the subsequent growth of NWs. Then NH_3 is introduced into the reactor without interrupting the N_2 flow in order to avoid the surface nitridation of Ga. The continuous supply of precursors leads to nucleation and subsequent growth of GaN NWs. In case of catalyst assisted GaN NWs (Ni and Au), both the precursors were introduced simultaneously since the initial Ga deposition step is not essential as the metal catalyst droplets activates the growth of NWs. The growth duration is fixed for one hour for all the samples. At the end, the reactor is turned off to cool down to room temperature naturally. All the growth parameters including flow rate, source to substrate distance, temperature and growth duration is kept constant for all the experiments.

The morphology and compositional variation of GaN NWs were studied using field emission scanning electron microscopy (FESEM) (Carl Zeiss - Σigma) equipped with energy dispersive X-ray analysis (EDX) (Oxford instruments). EDX has been recorded at 10 keV with the point resolution of around 10 nm. High resolution transmission electron microscope (HRTEM) (JEM 2010, JEOL, Japan) was carried out at an operating voltage of 200 kV to examine the crystallinity of a single GaN nanowire. The GaN nanowires were carefully removed from the Si substrate by the sonication process and then collected in the transmission electron microscopy (TEM) grid. Low temperature photoluminescence (PL) spectrum for the ensemble of NWs have been recorded by using the He-Cd laser of 325 nm (30mW) focused through a objective lens with the spot size of ~10 µm and the resulting luminescence signal has been collected through a monochromator (Horiba Jobin Yvon – 0.55 M) and a charge coupled device. The samples are placed in a closed cycle He cryostat with the temperature variable from 10 to 300 K.

Results and Discussion

Figure 1(a-f) show the electron microscopic images of self-catalytic assisted GaN NWs grown by chemical vapor deposition. Figure 1(a) shows the self-catalytic GaN NWs, with the average diameter and length of 150±20 nm and 1.8 µm, respectively. The average growth rate of NWs has been calculated to be 30 nm/min. For more electron microscopy images please refer supporting information S1. In the case of self-catalytic GaN NWs, the Ga metal droplet is normally not observed on the apex as the growth proceeds at higher temperature results in consumption or desorption of Ga.[30] Figure 1(b) shows TEM image recorded on the top part of a single GaN NW that reveals the absence of any such catalytic particle. Figure 1(c) shows the HRTEM image recorded on the top of the single GaN NW which contains defects such as stacking faults.[31] Figure 1(d) shows HRTEM recorded on the body of the single NW, which shows some extended defects.

Besides wurtzite structure, the presence of cubic inclusions and stacking faults is also evidenced by the corresponding selected area electron diffraction pattern (SAED) pattern (fig. 1(e)) taken from (0001) zone axis. HRTEM was recorded for several NWs and all the NWs show very similar defects for self-catalytic GaN NWs. The stacking faults and other defects in self-catalytic GaN NWs have been attributed to the change in supersaturation during the growth, despite the low growth rate.[32] HRTEM results reveal that the self-catalytic GaN nanowires contain defects and polycrystalline nature, which in turn affects the optical properties of the nanowires. However, deep investigations on the HRTEM analysis are required to map the defect formation and propagation which is beyond the scope of this manuscript. EDX recorded on the NWs shows slightly N rich conditions with the atomic ratio of 48.4: 51.6% for Ga and N, respectively. Here, the excess of N can be attributed to the N-rich growth conditions that favor the growth of anisotropic NWs under self-catalytic approach.

Figure 2(a) shows the tilt-view FESEM image of the high yield Ni-catalyst assisted GaN NWs. The average diameter and length of the NWs are 120 ±10 nm and 10 µm, respectively. Figure 2(b) shows the magnified view of single NW with the Ni-catalyst on the top of the NW. The calculated average axial growth rate is 165 nm/min. Figure 2(c) shows the low magnification HRTEM image recorded on the single NW which reveals that the NWs is long and straight with flat surface. In order to probe the crystalline nature of the catalytic alloy and GaN NWs HRTEM analysis has been carried out. Figure 2(c) presents a detailed HRTEM examination on the interface between the NW and the catalyst droplet of a single GaN NW which indicates that the interface is abrupt and smooth. Figure 2(d), the high magnification HRTEM image of a single NW shows free of domain boundaries and cubic inclusion having a single-crystalline nature. The crystalline nature of GaN NWs was further confirmed by SAED. Figure 2(e) shows SAED pattern, recorded perpendicular to the NW long axis.

This journal is © The Royal Society of Chemistry [year]

RSC Advances Accepted Manuscript

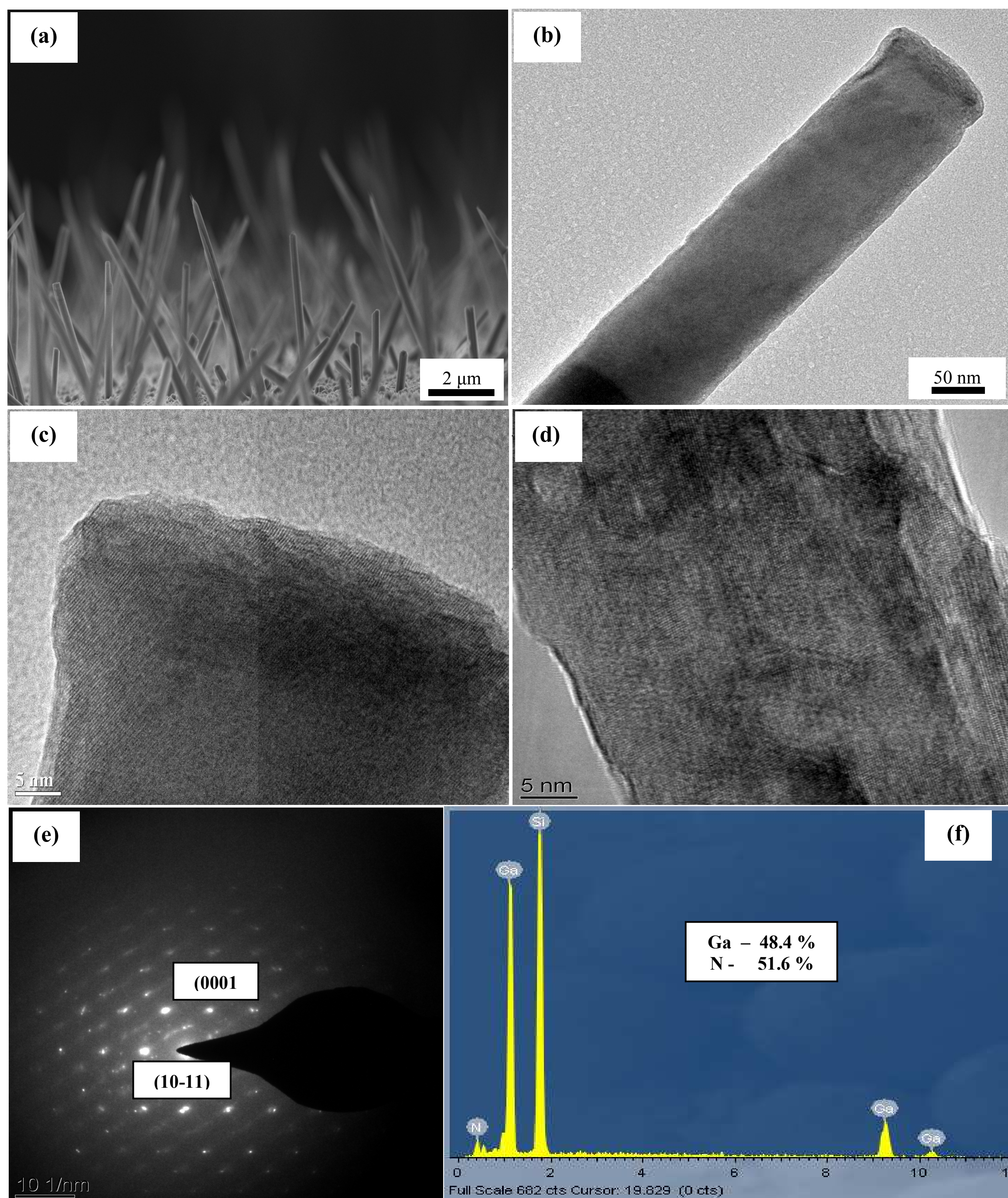

Figure 1: (a) shows the FESEM image of self-catalytic GaN NWs on Si (111) substrate, (b) Shows the TEM image of a single GaN NW and the top of the NW does not have any trace of catalyst particle, (c)-(d) HRTEM images of GaN NWs, (e) SAED pattern recorded on the body of a single GaN NW and (f) shows energy dispersive x-ray spectroscopy recorded on the ensembles of GaN NWs.

RSC Advances Accepted Manuscript

20

5

10

15

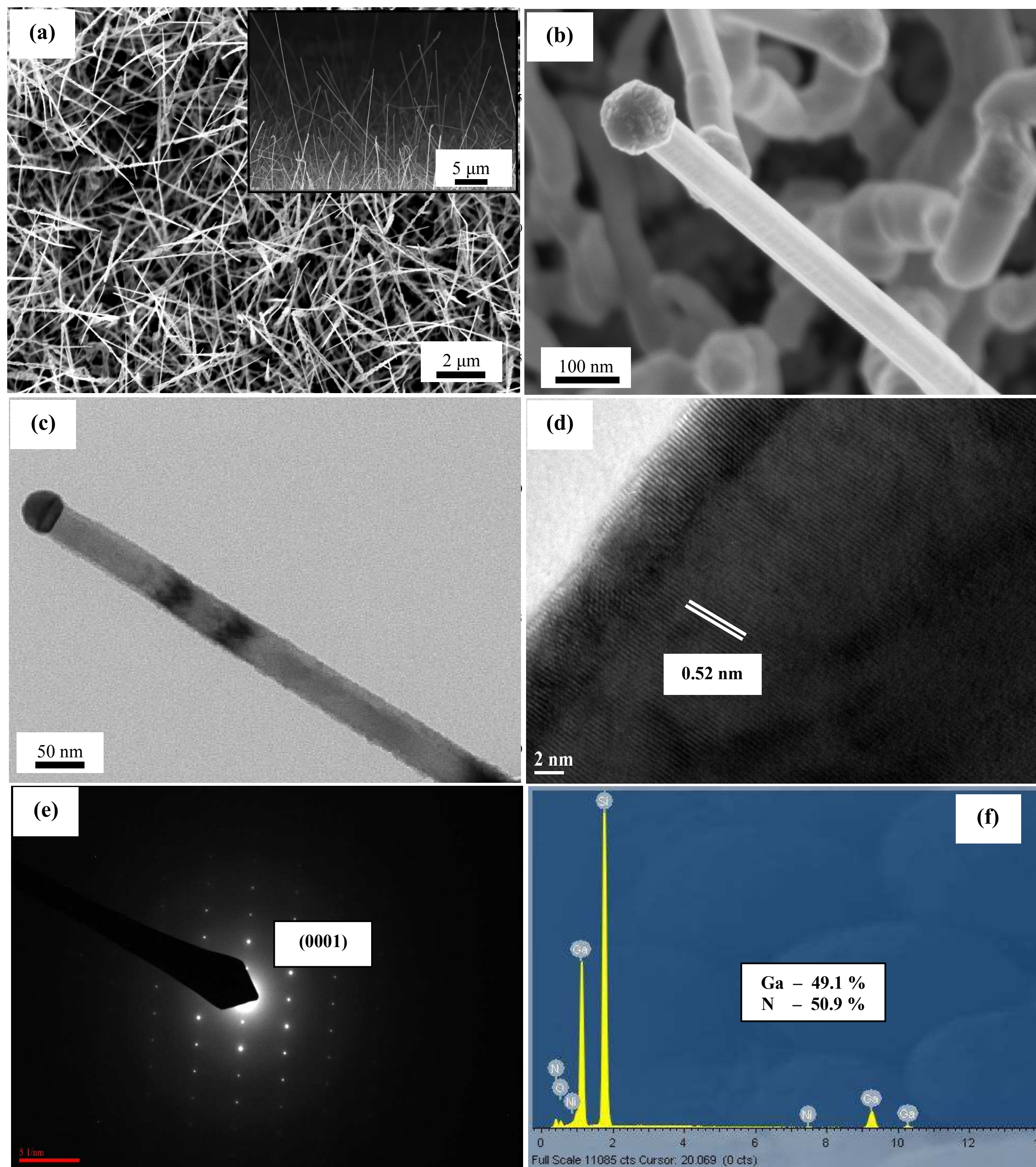

Figure 2: (a) shows the FESEM image of Ni-catalyst assisted GaN NWs on Si (111), inset shows the tilted view FESEM image (b) shows the magnified view on the top of the GaN NW, (c) shows TEM image of a single GaN NW, (d) HRTEM image recorded on the body of single GaN NW, (e) SAED pattern recorded on the body of NW and (f) EDX recorded on the ensembles of GaN NWs.

75

RSC Advances Accepted Manuscript

This journal is © The Royal Society of Chemistry [year]

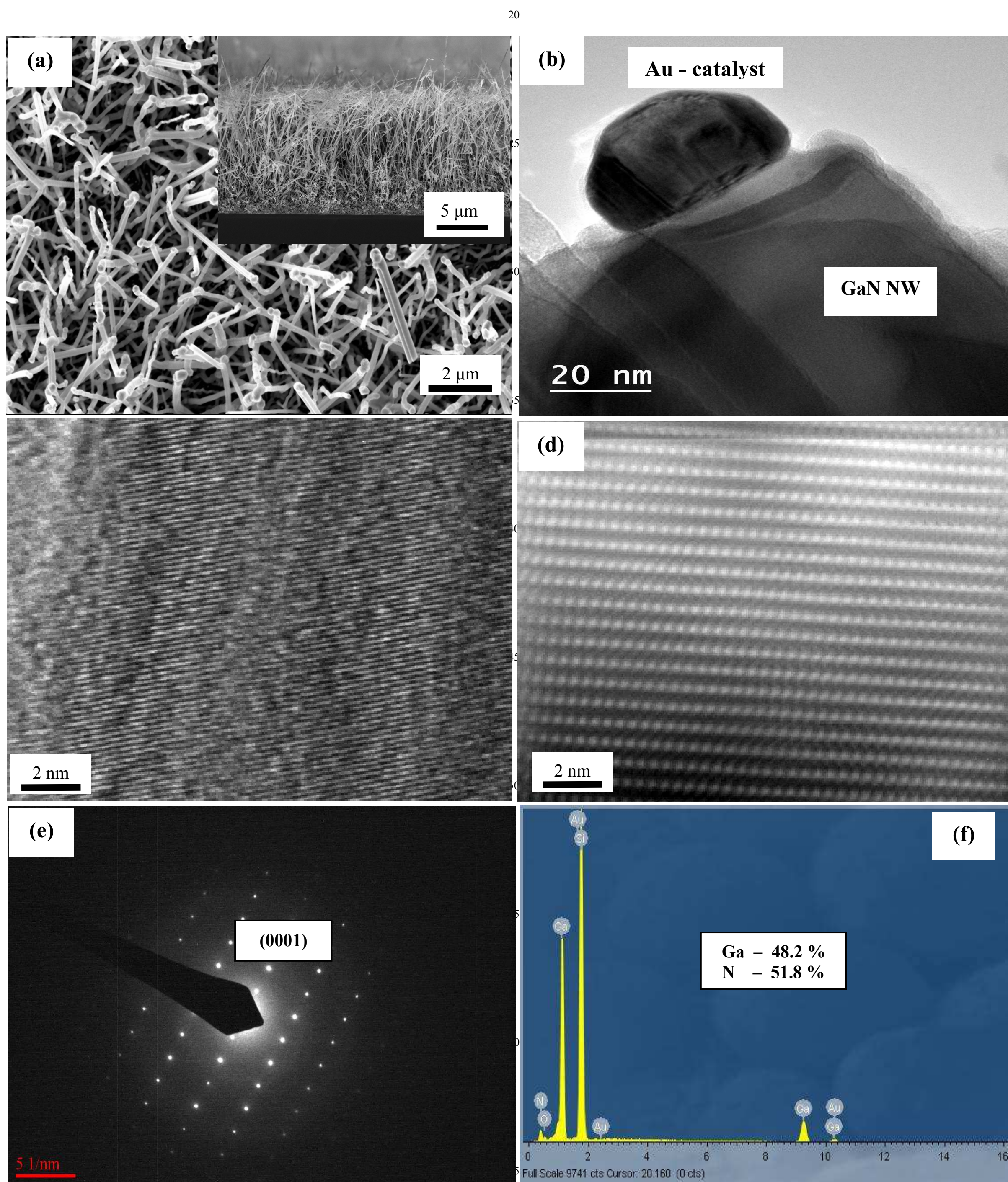

Figure 3: (a) shows the FESEM image of Au-catalyst assisted GaN NWs on Si (111), inset shows the tilted view FESEM image (b) Shows the TEM image of a single GaN NW, (c) shows HRTEM image of GaN NWs, (d) shows the FFT image of the same wire, (e) shows SAED pattern recorded on the body of NW and (f) EDX recorded on the ensembles of GaN NWs.

RSC Advances Accepted Manuscript

Detailed analysis of the diffraction pattern shows that the NW took the wurtzite structure and grew along c-direction. HRTEM and SAED observations over many NWs and also at different locations of each NW showed similar diffraction pattern and lattice fringes (d = 0.52 nm) oriented along (0001) crystallographic direction. A detailed analysis on the chemical composition of catalytic particle and the novel VLS approach in which the incorporation of Ga and N adatoms follows catalytic and triple phase boundary can be found elsewhere.[19] Unlike in MBE grown GaN NWs by Cheze et.al,[33] here the Ni assisted GaN NWs have high structural quality. In general, MBE grown NWs are often reported[34] to be superior to CVD grown. However, the poor quality of MBE grown Ni- catalyst assisted GaN NWs can be attributed to the low temperature growth at 730ºC whereas CVD GaN NWs were grown at 950ºC. Further, EDX recorded on the ensembles of GaN NWs shows almost equi-molar Ga to N ratio in addition to the presence of other elements such as Si, O and Ni as shown in figure 2(f). The presence of O from the elemental analysis has been attributed to the strong native oxide of Si substrate or the oxygen onto the ensembles of NWs during atmospheric transfer of samples for SEM imaging. Elemental analysis has also been carried out during the TEM analysis on single GaN NW which reveals the absence of O and Si impurities up to the detection limit.

Figure 3(a) shows the FESEM image of Au catalyst assisted GaN NWs. The average diameter and length of the NWs were 150 ±20 nm and 6 µm, respectively. The calculated average axial growth rate is 100 nm/min. There is no specific relationship can be established between the diameter and length (d vs. L) of the GaN nanowires for both catalyst and self-catalyst assisted growth of NWs. Figure 3(b-d) show the HRTEM images recorded on the body of the NW, which reveals that the NWs are free from defects such as cubic inclusion and having a single crystalline nature. The NW diameter is apparently very homogeneous from top to bottom without any tapering effect however branching and overlapping of NWs can be seen. Figure 3(d) shows the high-magnified HR-TEM lattice image of the NW taken normal to the growth axis. This image shows the (0001) growth direction of the NW. Lattice images of the NW are very clear without any vacancies defects and stacking faults. From the HR-TEM data, the interplanar spacing was observed to be ~0.51 nm. The crystalline nature of GaN NWs was further confirmed by SAED. Figure 3(e) shows SAED pattern, recorded perpendicular to the NW long axis. Elemental analyses carried out on the ensembles of NWs shows equi-molar ratio of Ga to N in addition to the presence of Si, O and Au. The structural quality of Au assisted GaN NWs and Ni assisted GaN NWs are very similar, which is in contradiction to the earlier report by Zhou et.al[35] in which they have shown that the Au assisted MOCVD grown GaN NWs contains basal stacking faults while the Ni assisted GaN NWs were free from such defects. Nevertheless, we attribute such quality difference may be due to the change in growth temperature along with the substrate effects, as they have[26] used r-plane sapphire substrate. It is worth to note that we have employed Si(111)-substrates for the fabrication of GaN NWs regardless of different catalyst. Seed particles, defects and compositional variations can strongly affect the NWs.[36,37]

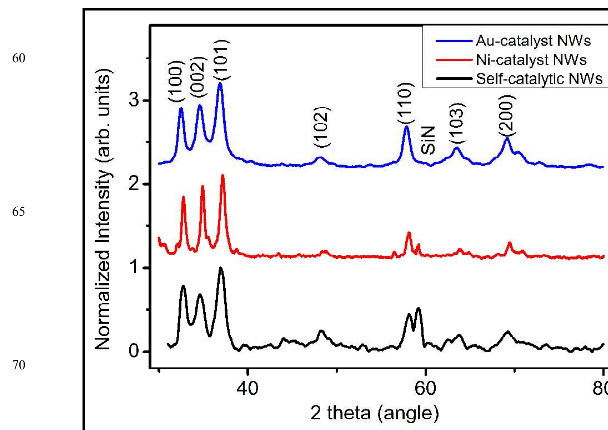

Figure 4 shows the XRD pattern recorded for the various types of catalyst and self-catalyst assisted GaN NWs.

Figure 4 shows the XRD pattern recorded for catalyst and self-catalyst assisted GaN NWs. All the diffraction peaks are well indexed to the wurtzite GaN (JCPDS Card No: 898624). The peak positions and their corresponding full width half maximum (FWHM) of dominant (100), (002) and (101) planes were shown in the supporting information S1. Ni-catalyst GaN NWs shows sharp diffraction peaks and evidently their FWHM values for (100), (002) and (101) planes are narrow as compared to Au-catalyst and self-catalyst GaN NWs. The above result clearly evidences high crystalline nature of Ni-catalyst GaN NWs. Despite poor crystalline nature of self-catalyst GaN NWs, the peak position of diffraction planes match well with the bulk GaN evidencing lattice relaxation. As the XRD pattern was recorded for the ensembles of GaN NWs, the diffraction from various hexagonal planes were also observed. The cubic and oxide phases were absent in all GaN NWs irrespective of growth process. However, the presence of weak SiN peak can be attributed to the nitridation of Si surface at growth temperature during initial stage of nucleation. To further investigate whether the optical properties of the GaN nanowires differ in growth using Au and Ni seed particles, or self catalyst, PL studies were performed on as-grown ensemble nanowires. Low temperature photoluminescence recorded at 10K for self-catalyst and catalyst assisted GaN NWs are shown in Figure 5. At first sight on the luminescence studies two important observations can be made. The first one is that self-catalytic GaN NWs contains defect related emission as compared with the catalyst assisted GaN NWs. The second one is that Ni assisted GaN NWs (figure 5) shows dominant emission around the GaN band edge without the yellow luminescence which is frequently observed in GaN thin films and nanowires. All the data for the comparison of luminescence properties of catalyst and self-catalyst NWs are given in Table 1.

Lorentzian peak fitted spectra of Ni, Au and self-catalytic GaN NWs recorded at 10 K show free donor bound exciton (D^0X) transitions at 3.485, 3.484 and 3.468 eV respectively, with the Full width at half maximum (FWHM) of 63.9, 74.7 and 122 meV. As the temperature increases, D^0X peak positions of Ni, Au and self-catalytic GaN NWs shift to lower energy and the peaks centered at 3.441, 3.440 and 3.407eV with the FWHM of 146, 148 and 178 meV, respectively for 300 K. The FWHM of the

 This journal is © The Royal Society of Chemistry [year]

RSC Advances Accepted Manuscript

D^0X peaks are higher as compared with the MOCVD[38] and MBE[39] grown NWs and it is likely because the PL spectra were taken on an ensemble of GaN nanowires. PL spectra were recorded for number of samples grown by both catalytic and self-catalytic assisted GaN NWs. None of the Ni-catalyst assisted GaN NWs exhibited the yellow band (YL@10K), which is an indication of very low defect densities. However YL band is clearly visible for Au-GaN NWs but dominantly present for self-catalytic GaN NWs.

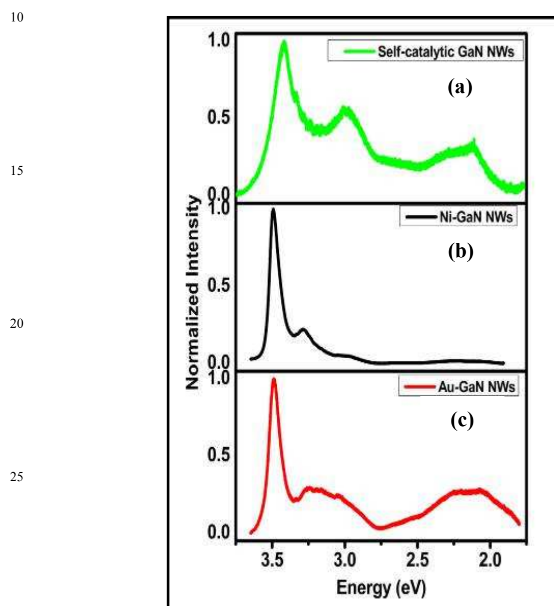

Figure 5: (a-c) show the photoluminescence spectra of GaN NWs recorded at 10K (a) Self-catalyst GaN NWs (b) Ni assisted GaN NWs and (c) Au assisted GaN NWs.

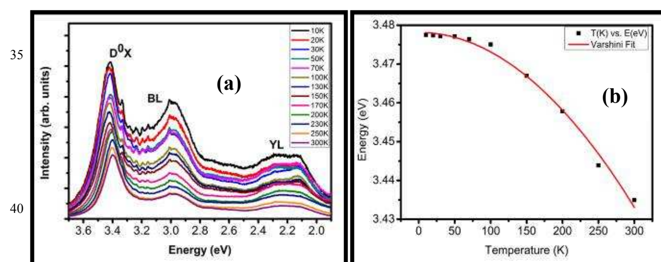

Figure 6: (a) shows temperature dependent photoluminescence spectrum recorded for self-catalytic GaN NWs for various temperature ranges and (b) shows its corresponding Varshni fitting.

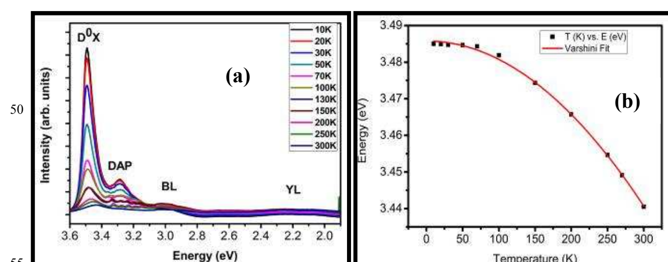

Figure 7: (a) shows temperature dependent photoluminescence spectrum recorded for Ni-catalyst assisted GaN NWs for various temperature ranges and (b) its corresponding Varshni fitting.

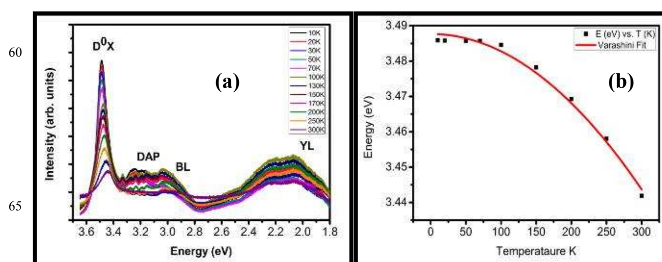

Figure 8: (a) shows temperature dependent photoluminescence recorded spectrum for Au-catalyst assisted GaN NWs for various temperature ranges and (b) shows its corresponding Varshni fitting.

As shown in Figure 5, a typical 10 K PL spectrum of Ni, Au and self-catalyzed GaN nanowires, all the NWs exhibited a strong ultraviolet emission besides deep level emission at 3.25-29 eV pertaining to shallow donor acceptor recombination (DAP).[40] DAP band of all NW samples shifts to higher energies (from 3.31 eV to 3.34 eV) with the increase of temperature due to the thermal escape of electrons from long-lived distant pairs contributing at the low-energy side of a PL band due to weaker Coulomb interaction.[41] The shallow DAP has been attributed [42] to defects such as Si_{Ga} and O_N as both the defects are quite possible in our growth approach. Si has high solubility in both Ni and Au, and hence the NWs can have Si interstitials and/or Si_{Ga} type defects. Further, it has been widely reported that the catalytic grown GaN NWs on Si substrates can be unintentionally doped with Si.[43] In addition with Si, oxygen could also be incorporated in to the growing NW from the native oxide layer of Si. The other source for oxygen could be from the atmospheric transfer of samples for analysis. EDX recorded for all the ensemble of NWs shows the small traces of oxygen with less than 1 at.% in all the cases and however elemental analysis carried out through TEM analysis does not show any traces of O in single GaN NW up to the detection limit.

At 10 K, GaN NWs samples exhibit blue band emission at 2.9-3.1 eV, owing to the transitions from the conduction band or a shallow donor to a relatively deep acceptor.[44] Especially self-catalytic GaN NWs shows dominant blue luminescence (BL) band at low temperature as compared with the Ni and Au assisted GaN NWs. The intensity of the BL band decreases with increasing temperature from 10 to 300 K and the quenching of the BL band at high temperature can be attributed to the escape of holes from the acceptor to the valence band and/or the bound holes may non-radiatively recombine with free electrons in the conduction band. However, in case of Ni and Au catalyst assisted GaN NWs the BL band increases with increasing temperature and shows opposite tendency to self-catalytic NWs. Generally the BL band is related to a shallow acceptor (Si_N or C_N) and the origin of this BL band is still a topic of considerable debate in literature.[38]

In most of the unintentionally and intentionally doped *n*-type GaN samples grown by the various techniques available, the room-temperature PL spectrum contains a near band- edge emission at about 3.42 eV and the YL band centering at 2.20–2.25 eV (Figure 6(a) 7(a) and 8(a)). Here, at 10 K the YL band was present in both the Au and self-catalytic NWs and the peak was too weak to be observed for Ni-GaN NWs. In case of catalytic NWs the YL band suppressed at low temperature and at

RSC Advances Accepted Manuscript

10 K, Ni assisted GaN NWs does not possesses any visible YL band. For self-catalytic GaN NWs YL band broadened (450 meV) and increases with temperature. The increase of YL band with temperature is typical for defects with strong electron-phonon coupling. There are several contradictory results in the literature concerning the origin of the YL band and the effects of doping on its intensity. First principle calculations predict[45] that several V_{Ga}-related defects may be responsible for YL in undoped GaN which confirm that the Ni-GaN NWs are free from the defects such as V_{Ga}, V_N and complex defects related that gives rise to emission at 2.2 eV.[28,29] This can be related to the high solubility of Ga in Ni-catalyst particle which continuously supply Ga-adatoms to the growth interface for the crystallization of GaN thereby reducing Ga-vacancy related defects.

Luminescence properties of NWs	D^0X		NBE		Defect levels		
	E (eV)	FWHM (meV)	E (eV)	FWHM (meV)	DAP at 300 K (eV)	BL at 300 K (eV)	YL at 300 K (eV)
Self catalytic NWs	3.468	127.4	3.407	174	3.20	3.07	2.22
Ni-GaN NWs	3.485	63.9	3.441	146	3.25	3.00	Nil
Au-GaN NWs	3.484	74.7	3.440	178	3.29	2.96	2.01

Table 1: Shows the emission characteristics of GaN NWs grown with different catalyst.

Further, the effective ionic radii of Ni (60 pm) is smaller than Ga 62 pm), thus the Ga vacancies can easily be replaced by the Ni ions. In generally, the Ga vacancies (negatively charged) and the Ni ions (3+) are in the opposite charge state. Hence, the suppression of YL band in Ni-GaN NWs can be ascribed to the compensation of deep level defects such as Ga vacancies.[46] However, deep investigations are warranted to confirm the presence of Ni in the lattice of GaN. Using the Varshni formula[47] and band-tail model, the temperature-dependent emission energy can be fitted by

$$E_g(T) = E_g(0) - \left(\frac{\alpha T^2}{T+\beta}\right) \quad \text{-------------- (1)}$$

where, E (0) is the emission energy at 0 K. α and β are fitting parameters to be determined by curve fitting to the experimental data. The results of the best fit are represented by red line. Figure 6(b), 7(b) and 8(b) shows the Varshni fitting for the energy of DBE peak at various temperatures. The fitting parameters for Ni, Au and self catalyst NWs (Table 1) are $E_g(0)$ =3.4876, 3.4857, 3.4681 eV , $\alpha = 1.19\times10^{-9}$, 1.10×10^{-9}, 9.21×10^{-8} eV K^{-1} and β =583, 561, 521 K, respectively. The estimated value of $E_g(0)$ for the free exciton emission for all the Ni- and Au catalyst samples agrees well with the reported value of wurtzite GaN.[48]

Summary

We have compared the structural and luminescence properties of GaN nanowires grown with different self-catalyst and catalyst approach. The self-catalytic GaN NWs contain high density of structural defects such as stacking faults and cubic inclusions whereas Ni and Au catalyst GaN NWs possesses high structural quality along with the absence of such defects. The PL spectra of the self-catalytic GaN NWs exhibit defects related BL and YL band in addition to the broad band edge emission. For Ni and Au assisted GaN NWs the PL emission is much stronger with donor bound exciton at ~ 3.485 eV. Further, Ni-GaN NWs does not have any visible YL band demonstrating superior structural and optical quality over Au and self catalytic GaN NWs. The poor optical quality of CVD grown self-catalytic GaN NWs has been attributed to the presence of defects and structural disorder as evidenced by the electron microscopy.

Acknowledgements

One of the authors K.J thanks Department of Science and Technology (DST), Govt. of India for the financial assistance under the Nanomission project No. SR/NM/NS-77/2008. V.P acknowledges CSIR, Govt. of India for the award of senior research fellowship (SRF).

Notes and references

a. *Centre for Nanoscience and Nanotechnology, School of Physics, Bharathidasan University, Tiruchirappalli, 620024, India.*
b. *Semiconductor Materials Process Laboratory, School of Advanced Materials Engineering, Engineering College, Research Center for Advanced Materials Development (RCAMD), Chonbuk National University, Deokjin-dong 664-14, Chonju 561-756, Korea*

Corresponding author Email – kjeganathan@yahoo.com

1 Y. Li, J. Xiang, F. Qian, S. Gradecak, Y. Wu, H. Yan, D. A. Blom, C. M. Lieber, Nano Lett. 2006, **6**, 1468-1473.
2 F. A. Ponce, D. P. Bour, Nature (London) 1997, **386**, 351−359.
3 J. W. Orton, C. Foxon, Rep. Prog. Phys. 1998, **61,** 1-75.
4 H. M. Kim, Y. H. Cho, H. Lee, S. I. Kim, S. R. Ryu, D. Y. Kim, T. W. Kang, K. S. Chung, Nano Lett. 2004, **4,** 1059-1064.
5 X. Duan, C. M. Lieber, J. Am. Chem. Soc. 2000, **122**, 188−189.
6 S. Y. Bae, H. W. Seo, J. Park, H. Yang, J. C. Park, S. Y. Lee, Appl. Phys. Lett., 2002, **81**, 126.
7 Z. J. Li, X. L. Chen, H. J. Li, Q. Y. Tu1, Z. Yang, Y. P. Xu, B. Q. Hu, Appl. Phys. A: Mater. Sci. Process. 2001, **72**, 629-632.
8 R. S. Wagner, W. C. Ellis, Appl. Phys. Lett., 1964, **4,** 89.
9 A. I Persson, M .W. Larsson, S. Stenstrom, B. J. Ohlsson, L. Samuelson, L. R. Wallenberg, Nat. Mater., 2004, **3**, 677–681.
10 A. J. Tavendale and S. J. Pearton, J. Phys. C: Solid State, Phys., 1983, 16, 1665.
11 K. A. Dick and P. Caroff, Nanoscale, 2014, 6, 3006-3021.
12 J. E. Allen, E. R. Hemesath, D. E. Perea, J. L. Lensch-Falk, S. Y. Li, F. Yin, M. H. Gass, P. Wang, A. L. Bleloch, R. E. Palmer, Nat. Nanotechnol. 2008, **3**, 168−173.

RSC Advances Accepted Manuscript

This journal is © The Royal Society of Chemistry [year]

13 R. Q. Zhang, Y. Lifshitz, S. T. Lee, Adv. Mater. **15**, 635–640, 2006.
14 J. Noborisaka, J. Motohisa, T. Fukui, Appl. Phys. Lett. 2005, **86,** 213102.
15 M. He, I. Minus, P. Zhou, S. N. Mohammed, J. B. Halpern, R. Jacobs, W. L. Sarney, L. S. Riba, R. D. Vispute, Appl. Phys. Lett., 2000, **77**, 3731.
16 B. Mandl, J. Stangl, T. Mårtensson, A. Mikkelsen, J. Eriksson, L. S. Karlsson, G. Bauer, L. Samuelson, W. Seifert, Nano Lett. 2006, **6**, 1817–1821.
17 P. J. Poole, J. Lefebvre, and J. Fraser, Appl. Phys. Lett., 2003, **83**, 2055.
18 E. Stach, P. Pauzauskie, T. Kuykendall, J. Goldberger, R. He, and P. Yang,Nano Lett., 2003, **3**, 865.
19 Y. Zhang, H. Jia, and D. Yu, J. Phys. D, 2004, **37**, 413.
20 C. J. Novotny and Paul K. L. Yu, Appl. Phys. Lett., 2005, **87**, 203111.
21 V. Purushothaman, V. Ramakrishnan, K. Jeganathan, RSC Adv. 2012, **2**, 4802−4806.
22 C. Colombo, D. Spirkoska, M. Frimmer, G. Abstreiter, and A. Fontcuberta i Morral, Phys. Rev. B, 2008, **77**, 155326.
23 A. Fontcuberta i Morral, C. Colombo, G. Abstreiter, J. Arbiol and J. R. Morante, Appl. Phys. Lett., 2008, **92**, 063112.
24 F. Jabeen, V. Grillo, S. Rubini and F. Martelli, Nanotechnology, 2008, **19,** 275711.
25 J. Noborisaka, J. Motohisa, and T. Fukui, Appl. Phys. Lett., **86**, 2005, 213102.
26 V. Purushothaman, V. Ramakrishnan, K. Jeganathan, CrystEngComm, 2012, 14, 8390–8395.
27 V. Purushothaman, K. Jeganathan, J. Phys. Chem. C. 2013, **117**, 7348−7357.
28 C. Chèze, L. Geelhaar, O. Brandt, W. M. Weber, H. Riechert, S. Münch, R. Rothemund, S. Reitzenstein, A. Forchel, T. Kehagias, P. Komninou, G. P. Dimitrakopulos, T. Karakostas, Nano Res. 2010, **3**, 528–536.
29 V. Purushothaman, K. Jeganathan, J. Nanopart. Res. 2013, **15**, 1789.
30 J. Noborisaka, J. Motohisa, T. Fukui, Appl. Phys. Lett. 2005, **86**, 213102.
31 D. Tham, C. Y. Nam, J. E. Fischer, Adv. Funct. Mater. 2006, **16**, 1197.
32 N. A. Jeon, S. A. Dayeh, L. J. Lauhon, *Nano Lett.*, 2013, **13(8),** 3947–3952.
31 C. Chèze, L. Geelhaar, O. Brandt, W. M. Weber, H. Riechert, S. Münch, R. Rothemund, S. Reitzenstein, A. Forchel, T. Kehagias, P. Komninou, G. P. Dimitrakopulos, T. Karakostas, Nano Res. 2010, **3**, 528–536.
34 C. Chèze, L. Geelhaar, B. Jenichen, H. Riechert, Appl. Phys. Lett. 2010, **97**, 153105.
33 X. Zhou, J. Chesin, S. Crawford, S. Gradecak, Nanotechnology. 2012, **23**, 285603.
36 M. M. Brewster, X. A. Zhou, S. K. Lim, S. Gradecak, J. Phys. Chem. Lett. 2011, **2**, 586.
37 S. K. Lim, S. Crawford, G. Haberfehlner, S. Gradecak, Nano Lett., 2013, **13(2),** 331–33.
38 A. A. Talin, G. T. Wang, E. Lai, R. J. Anderson, Appl. Phys. Lett. 2008, **92**, 093105.
39 N. Thillosen, K. Sebald, H. Hardtdegen, R. Meijers, R Calarco, S. Montanari, N. Kaluza, J. Gutowski, H. Lüth, Nano Lett., 2006, **6(4),** 704–708.
40 M. C. Reshchikov, H. Morkoç, J. Appl. Phys. 2005, **97**, 061301.
41 D. G. Thomas, J. J. Hopfield, W. M Augustyniak, Phys. Rev. 1965, **140**, 202.
42 S. M. Lee, M. A. Belkhir, X. Y. Zhu, Y. H. Lee, Y. G. Hwang, T. Frauenheim, Phys. Rev. B. 2000, **61**, 16033.
43 J. Liu, X. M. Meng, Y. Jiang, C. S. Lee, I. Bello, S. T. Lee, Appl. Phys. Lett. 2003, **83**, 4241.
44 A. Y. Polyakov, M. Shin, J. A. Freitas, Jr. M. Skowronski, D. W. Greve, R. G. Wilson, J. Appl. Phys.1996, **80**, 6349.
45 C. G. Van de Walle, J. Neugebauer, J. Appl. Phys. 2004, **95,** 3851.
46 G. Devaraju, A.P. Pathak, N. Srinivasa Rao, V. Saikiran, Francesco Enrichi, Enrico Trave, Nucl. Instrum Meth B, 2011, **269**, 1925–1928.
47 V. P. Varshni, Physica, 1967, 149-154.
48 M. O. Manasreh, Phys. Rev. B, 1996, **53**, 16425-16428.

RSC Advances Accepted Manuscript